Proceedings of the ASME 2007 Summer Bioengineering Conference (SBC2008)
June 25-29, Marriott Resort, Marco Island, Florida, USA

SBC2008-192890

AN ANISOTROPIC HYPERELASTIC MODEL APPLIED TO NONDEGENERATE AND DEGENERATE ANNULUS FIBROSUS

Grace D. O'Connell (1, 2), Heather L. Guerin (3), Dawn M. Elliott (1, 2)

(1) McKay Orthopaedic Research Laboratory,
Department of Orthopaedic Surgery,
University of Pennsylvania
Philadelphia, PA

(2) Department of Bioengineering,
University of Pennsylvania
Philadelphia, PA

(3) Exponent, Inc. Philadelphia, PA

INTRODUCTION

The intervertebral disc is comprised of complex components that provide the disc with nonlinear, viscoelastic and anisotropic mechanical properties. The annulus fibrosus (AF) is a highly organized structure composed of concentric layers of collagen fibers embedded in a proteoglycan matrix. The AF has a high tensile stiffness and supports the large loads encountered by the disc. Mathematical models are needed to interpret and elucidate the meaning of experimental measurements made in mechanical tests. Based upon the classic work of Spencer [1], the AF has been modeled as a fiber-induced anisotropic hyperelastic material [e.g.,2-6], using the principle invariants of the Green deformation tensor and structural tensors representing the collagen fiber populations. Contributions of other AF components to mechanical behaviors are less understood than the fibers or matrix and may include connections between collagens and proteoglycans that can be incorporated into models through fiber-matrix interactions [2-4]. The previous models, however, have not been applied to experimental data from both nondegenerate and degenerate tissue. Constitutive modeling applied to nondegenerate and degenerate AF may elucidate microstructural changes with degeneration, will be useful for finite element models [5], and provide targets for disc treatments, such as tissue engineered constructs [7].

A previous study in our laboratory derived a nonlinear, anisotropic, hyperelastic model, which described the AF tissue using strain energy equations for the collagen fibers, extracellular matrix, and fiber-matrix interactions (FMI) [2]. The objective of this study was to use an updated version of the established model to describe the behavior of both nondegenerate and degenerate AF tissue, using uniaxial tensile experimental data. Furthermore, the model was used to determine the stress contribution by each component and evaluate the changes with degeneration.

METHODS AND MATERIALS

Mechanical Testing:

Intervertebral discs from the L3-L4 and the L4-L5 levels were dissected from seven human cadavaric lumbar spines, as previously described [8]. Samples were graded using the Thompson scale, with grades below 2.5 considered nondegenerate (n = 7, age 36-53 years old) and greater than 2.5 as degenerate (n = 5, age 53-80 years old). Samples were prepared from the outer AF, oriented along the circumferential and radial directions (length x width x thickness: 15.8 x 2.8 x 1.9 mm & 14.0 x 2.5 x 1.8 mm, respectively). Samples were preconditioned and stretched in a uniaxial quasi-static ramp test, with optical images acquired to measure two-dimensional Lagrangian tissue strains [5]. The components of the right Cauchy-Green deformation tensor (**C**) were calculated from measured Lagrangian strains, and the 2nd Piola-Kirchhoff stress (**S**) was calculated from the measured Lagrangian stress. Multidimensional datasets were constructed using the stress and strain data from matched circumferential and radial samples. The dataset was comprised of stress and strain components measured in the loading direction, and transverse and out-of-plane strains calculated using sample-specific Poisson's ratio.

Constitutive Modeling:

A structurally motivated anisotropic hyperelastic model with finite deformations was formulated based upon the work of Spencer [1] and as previously published [2]. The strain energy function was described as a combination of each structural component using the integrity basis of invariants, formed from the deformation tensor **C** and the unit fiber direction vectors **a** and **b**: $I_1 = trC$, $I_2 = 1/2[(trC)^2 - trC^2]$, $I_3 = \det C$, $I_4 = a \cdot C \cdot a, I_5 = a \cdot C^2 \cdot a$, $I_6 = b \cdot C \cdot b$, $I_7 = b \cdot C^2 \cdot b$. The matrix stain energy (W_m) was described as a compressive Mooney-Rivlin

material and the fiber strain energy (W_f) was described using an exponential [2, 5].

$$W_m = c_1(I_1 - 3) + c_2(I_2 - 3) + c_3(J-1)^2 + (c_1 + 2c_2)\ln J$$

$$W_f = \sum_{\alpha = 4,6} \frac{c_4}{2c_5}\left(e^{c_5(I_\alpha - 1)^2} - 1\right)$$

The shear fiber-matrix interaction (FMI) represents energy transfer parallel to the fibers. The shear FMI strain energy ($W_{shearFMI}$) was described using a three-dimensional rotation of the material line element parallel to the fiber direction modified from the equation proposed by Peng et al [4].

$$W_{shearFMI} = \sum_{\alpha = 4,6}\left(c_6\left(\frac{I_\alpha}{I_3}(I_5 - I_1 I_\alpha + I_2) - 1\right)^2\right)$$

The strain energy equations were differentiated with respect to the deformation tensor to obtain stress: $\mathbf{S} = 2\delta W/\delta C$. The model was fit to the experimental data to determine the model parameters, c_1-c_6, as follows. Radial experimental data were fit first using the stress-stretch equation derived from the W_m, to determine c_1-c_3. Then, the stress-stretch equation derived from the full strain energy equation ($W = W_m+W_f+W_{shearFMI}$) was fit to the circumferential data and the matrix constants to determine c_4-c_6. A least-squares solution to the general linear model was implemented to find the best-fit model parameters.

The contribution of each component to the overall stress was determined for the toe- and linear-regions of the circumferential stress-stretch curve. An unpaired Student's t-test was performed to compare nondegenerate and degenerate mechanical properties and model parameters, and the stress contribution from the toe- and linear-regions was compared using a paired t-test, with significance set at $p \leq 0.05$.

RESULTS

The radial direction stress-stretch behavior of the nondegenerate sample exhibited nonlinear behavior, while the degenerate tissue exhibited linear behavior; both were well-described by the Mooney-Rivlin model ($R^2 = 0.94$, Fig 1A). For nondegenerate AF, the toe- and linear-region modulus and the Poisson's ratio were 0.14 ± 0.05 MPa, 0.30 ± 0.11 MPa and 0.86 ± 0.40, respectively. For degenerate AF, the linear-region modulus and Poisson's ratio were 0.43 ± 0.18 MPa and 0.57 ± 0.38, respectively, with no significant differences compared to nondegenerate. The model parameters are provided in the Table. While no significant differences were observed with degeneration for c_2 and c_3, there was a 3X increase in c_1 with degeneration ($p < 0.05$).

The circumferential direction nondegenerate toe- and linear-region modulus and the Poisson's ratio were 2.59 ± 1.93 MPa, 34.3 ± 27.3 MPa and 2.65 ± 1.31, respectively. For degenerate AF, the toe- and linear-region modulus and Poisson's ratio were 4.31 ± 3.20 MPa, 35.0 ± 23.3 MPa and 2.39 ± 1.76, respectively, with no significant differences compared to nondegenerate. The strain energy equation fit well to the circumferential data, $R^2 = 0.99$ (Fig 1B). While there was no effect with degeneration for the fiber terms, c_4 and c_5, there was a 4X increase in the shear FMI term, c_6, with degeneration ($p < 0.05$, Table).

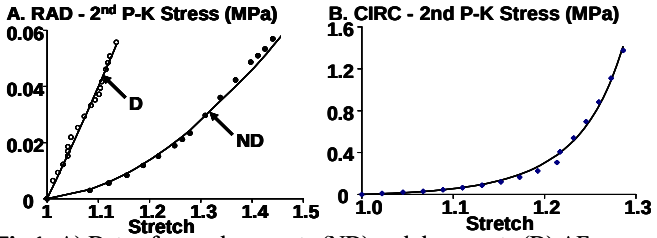

Fig 1: A) Data of a nondegenerate (ND) and degenerate (D) AF tissue along the radial direction and B) the same ND sample along the circumferential direction. The model fit is shown by the solid line.

	c_1 (Mpa)	c_2 (Mpa)	c_3 (Mpa)	c_4 (Mpa)	c_5	c_6 (Mpa)
Non-degenerate	*0.10 (0.08)	-0.12 (0.13)	0.11 (0.13)	0.14 (0.16)	39.1 (34.5)	* 29.9 (31.6)
Degenerate	*0.27 (0.17)	-0.20 (0.17)	0.26 (0.39)	0.95 (1.19)	12.2 (17.1)	*110.5 (54.2)

Table: Model parameters, average (std deviation), * $p < 0.05$

In the toe-region of AF oriented along the circumferential direction, the fiber stretch was responsible for the greatest proportion of stress, followed by the shear FMI, and the matrix contributed the least (Fig 2A). There was no difference with degeneration in relative stress contributions observed in the toe-region (Fig 2A). In the linear-region, variations were observed with degeneration. In nondegenerate tissue, the fibers stretch had the greatest proportion of total stress, followed by the shear interaction term, and the matrix contributed the least (Fig 2B). However, in degenerate tissue, the shear interaction term was responsible for the greatest proportion of stress, followed by the fibers and then the matrix. A 30% decrease was observed in the matrix contribution from the toe- to the linear-region for both nondegenerate and degenerate discs ($p < 0.01$).

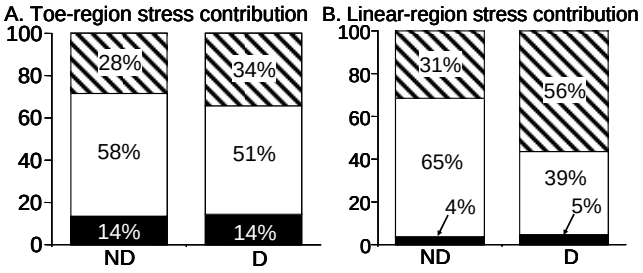

Fig 2: Stress contribution of samples oriented in the circumferential direction for the A) toe- and B) linear-region. Components include the ■ matrix, □ fibers, and the ▨ shear FMI.

DISCUSSION

The most important finding in this study was that the structurally motivated anisotropic hyperelastic model was able to detect changes with degeneration in AF mechanical function even though the bulk AF tissue tensile properties were not significantly altered with degeneration. The model detected differences in the matrix parameter (c_1) and the shear FMI parameter (c_6), suggesting changes with degeneration at the microstructural level.

This study also elucidated the relative role of the matrix, fibers, and FMI in nondegenerate and degenerate AF tissue in circumferential tension. While the fibers contributed to the largest proportion of the linear-region stress in nondegenerate AF tissue, the shear FMI component had a larger contribution in degenerate AF. This may be due to an increase number of collagen crosslinks or elastin or other compositional and structural changes that occur with degeneration. The contribution of the matrix diminished from the toe- to the linear-region. This was expected as the collagen fibers become more engaged in the linear-region of the stress-strain response.

This study improved upon the previous model in our laboratory by constraining the fibers from being loaded in compression (I_4 & $I_6 \geq 1$). A term describing the normal FMI [2, 6] was not included in this model, as this term was either 0 or negative when included.

REFRENCES

[1] Spencer 1984, [2] Guerin JOR 2007, [3] Wagner JOR 2004, [4] Peng J Appl Mech 2006, [5] Eberlein Comp Mech 2004, [6] Wagner J Biomech 2006, [7] Nerurkar JOR 2007, [8] Guerin J Biomech 2006

ACKNOWLEDGEMNETS

Supported by the NIH (EB02424) and the Penn Center for Musculoskeletal Disorders. Human tissue was obtained from NDRI.